Integrin $\alpha_v\beta_3$ on human endothelial cells binds von Willebrand factor strings under fluid shear stress

Jing Huang,[1] Robyn Roth,[2] John E. Heuser,[2] and J. Evan Sadler[1]

[1]Departments of Medicine, Biochemistry and Molecular Biophysics, and Howard Hughes Medical Institute, and [2]Department of Cell Biology, Washington University School of Medicine, St Louis, MO

Acutely secreted von Willebrand factor (VWF) multimers adhere to endothelial cells, support platelet adhesion, and may induce microvascular thrombosis. Immunofluorescence microscopy of live human umbilical vein endothelial cells showed that VWF multimers rapidly formed strings several hundred micrometers long on the cell surface after stimulation with histamine. Unexpectedly, only a subset of VWF strings supported platelet binding, which depended on platelet glycoprotein Ib. Electron microscopy showed that VWF strings often consisted of bundles and networks of VWF multimers, and each string was tethered to the cell surface by a limited number of sites. Several approaches implicated P-selectin and integrin $\alpha_v\beta_3$ in anchoring VWF strings. An RGDS peptide or a function-blocking antibody to integrin $\alpha_v\beta_3$ reduced the number of VWF strings formed. In addition, integrin α_v decorated the VWF strings by immunofluorescence microscopy. Furthermore, lentiviral transduction of shRNA against the α_v subunit reduced the expression of cell-surface integrin $\alpha_v\beta_3$ and impaired the ability of endothelial cells to retain VWF strings. Soluble P-selectin reduced the number of platelet-decorated VWF strings in the absence of Ca^{2+} and Mg^{2+} but had no effect in the presence of these cations. These results indicate that VWF strings bind specifically to integrin $\alpha_v\beta_3$ on human endothelial cells. (Blood. 2009;113:1589-1597)

Introduction

von Willebrand factor (VWF) is a multimeric plasma glycoprotein that plays an important role in hemostasis and thrombosis, primarily by interacting with platelet adhesion receptors.[1] VWF is synthesized by vascular endothelial cells and megakaryocytes, and so-called ultralarge (UL) VWF multimers are stored in endothelial Weibel-Palade bodies and platelet α-granules for later secretion.[2,3] After secretion, some ULVWF remains on the cell surface as very long strings that become decorated with platelets. Eventually, ULVWF multimers are converted into smaller, less thrombogenic fragments by the metalloprotease ADAMTS13, which cleaves the Tyr1605-Met1606 bond in the central A2 domain of VWF.[4,5]

Unlike VWF in solution, which interacts weakly with platelets, surface-immobilized VWF strings spontaneously mediate platelet adhesion under fluid shear stress in vitro or in vivo. For example, platelets bind to VWF on cultured human umbilical vein endothelial cells (HUVECs) to form "beads-on-a-string" structures under laminar flow, and these structures are attached to the cell surface at relatively few discrete sites and are disrupted by plasma or recombinant ADAMTS13.[5-7] Studies using intravital microscopy in mice also found that platelets adhere to VWF strings on the endothelium of mesenteric venules within seconds after endothelial stimulation, and ADAMTS13 deficiency prolongs these VWF-mediated platelet-endothelial cell interactions.[8,9]

The molecules responsible for the attachment of VWF strings to endothelial cells have not been identified conclusively and may differ between species. During VWF biosynthesis, the D′D3 region of the VWF subunit binds to the integral membrane protein P-selectin and recruits it to Weibel-Palade bodies.[10] In addition, soluble P-selectin and antibodies to P-selectin were reported to block the formation of platelet-VWF strings on cultured HUVECs in a flow chamber, implicating P-selectin in the attachment of platelet-VWF complexes to the endothelial surface. RGDS peptide did not impair the formation of platelet-VWF strings, suggesting that integrin $\alpha_v\beta_3$ does not participate.[11] However, intravital microscopy in genetically modified mice indicated that neither P-selectin nor integrin $\alpha_v\beta_3$ is necessary to form platelet-VWF strings on mouse venules.[12]

To address the nature of VWF-endothelial interactions that are critical for primary hemostasis in human vasculature, we have reexamined the role of P-selectin and integrin $\alpha_v\beta_3$ in the attachment of VWF strings to cultured HUVECs under flow. By immunofluorescence and phase-contrast microscopy of both VWF and platelets on living cells, we found that only a subset of VWF strings can support platelet binding. In addition, VWF strings bind to the endothelial surface through discrete adhesion sites, some at the termini and some at internal locations on the VWF multimers. In contrast to previous studies, peptide and antibody inhibition assays, as well as RNA interference (RNAi) knockdown analysis, indicate that integrin $\alpha_v\beta_3$ stabilizes VWF strings. Our findings delineate a mechanism for specific and dynamic interactions between acutely secreted VWF and human endothelial cells.

Methods

Cells and reagents

HUVECs were purchased from Lonza Walkersville (Walkersville, MD) or collected from human umbilical veins[13] under a protocol reviewed and approved by the Washington University Human Research Protection Office.

Submitted May 20, 2008; accepted September 24, 2008. Prepublished online as *Blood* First Edition paper, October 16, 2008; DOI 10.1182/blood-2008-05-158584.

An Inside *Blood* analysis of this article appears at the front of this issue.

The online version of this article contains a data supplement.

The publication costs of this article were defrayed in part by page charge payment. Therefore, and solely to indicate this fact, this article is hereby marked "advertisement" in accordance with 18 USC section 1734.

HUVECs were cultured in endothelial growth medium-2 media supplemented with growth factors (Lonza Walkersville). U937 is a human lymphoma cell line with monocytic characteristics[14] that expresses the P-selectin ligand PSGL-1. U937 cells were cultured in RPMI 1640 medium (Sigma-Aldrich, St Louis, MO) supplemented with 10% fetal bovine serum. Human integrin $\alpha_v\beta_3$ antibody LM609 (function blocking),[15] α_v antibody LM142 (nonfunction blocking),[15] and α_5 antibody CBL497 were obtained from Chemicon International (Temecula, CA). Antibody 6D1 against platelet GpIbα was obtained from Dr Barry Coller (Rockefeller University, New York, NY).[16] Peptides with the sequences RGDS[17] and DELPQLVTLPHPNLHGPEILDVPST (fibronectin type III connecting segment fragment 1-25; CS-1 peptide),[18] and puromycin were obtained from Sigma-Aldrich. Fibrillar collagen and formalin-fixed platelets were purchased from Helena Laboratory (Beaumont, TX). Purified recombinant soluble P-selectin was obtained from R&D Systems (Minneapolis, MN). Anti–P-selectin monoclonal antibody S12[19] and P-selectin goat polyclonal antibody[20] were provided by Dr Rodger P. McEver (University of Oklahoma, Oklahoma City, OK).

Visualization and quantitation of VWF strings in parallel plate flow chambers

Perfusion assays were carried out in a parallel plate flow chamber (Glycotech, Gaithersburg, MD), which consists of a flow deck, a rubber gasket, and a collagen-coated glass coverslip with HUVECs (passage 2-5) grown to a confluent monolayer. Within a given experiment, the HUVECs used were from the same stock, plated on the same day, grown to confluence, and used to collect data within a few hours on a single day. Polyclonal rabbit antihuman VWF antibody (Dako North America, Carpinteria, CA) was conjugated to Alexa Fluor 594 using Zenon Alexa Fluor 594 rabbit IgG labeling kit (Invitrogen, Carlsbad, CA) according to the manufacturer's instructions. Perfusion buffer was supplemented with 2% bovine serum albumin (BSA), 100 μM histamine, fluorescent VWF antibody, and other components as indicated. Unless otherwise noted, perfusion buffer is medium 199 that contains $CaCl_2$ and $MgCl_2$, and flow rate was adjusted with a syringe pump (Harvard Apparatus, Holliston, MA). Time-lapse images were collected 5 minutes after the initiation of laminar flow, using an Axiovert 200M inverted microscope with a 40×/0.55 NA objective, standard filter sets, a CCD camera, and Axiovision software (Carl Zeiss, Thornwood, NY).

To quantitate VWF strings, 10 images of confluent HUVECs corresponding to 10 consecutive optical fields (400 × magnification) were chosen for each perfusion condition. Fluorescent VWF strings and platelet strings in each field were counted, excluding strings shorter than 20 μm. Differences between mean values were assessed for significance using the Student *t* test.

Immunofluorescence microscopy

Confluent HUVECs on glass-bottomed dishes (MatTek, Ashland, MA) were incubated with endothelial growth medium-2 medium containing 100 μM histamine (Sigma-Aldrich) for 30 minutes at 37°C. Cells were then washed with Dulbecco phosphate-buffered saline without Ca^{2+} or Mg^{2+} (DPBS) and fixed with 2% paraformaldehyde for 10 minutes. Alternatively, HUVECs on collagen-coated cover glasses were exposed to laminar flow for 5 minutes in the presence of 100 μM histamine. Cover glasses were carefully removed from the flow deck and placed in fixation buffer (2% paraformaldehyde in DPBS). In either case, fixed cells were blocked with DPBS containing 2% BSA for 30 minutes at room temperature. Cell-surface VWF was detected by incubation with human VWF polyclonal antibody (Dako North America) diluted 1:1000, followed by Alexa Fluor 594-labeled goat antirabbit IgG (Invitrogen) diluted 1:200 for 30 minutes. Integrin α_v was detected with mouse monoclonal antibody (LM142; Chemicon International) diluted 1:200 for 45 minutes, and subsequent incubation with Alexa Fluor 488–labeled antimouse IgG antibody (Invitrogen) diluted 1:200 for 30 minutes. Images were acquired with standard filter sets using an Axiovert 200M inverted microscope (Carl Zeiss). Antibody LM142 gave no fluorescence signal for CHO-K1 cells, which do not express integrin α_v (Figure S1, available on the *Blood* website; see the Supplemental Materials link at the top of the online article).

Photoshop CS3 (Adobe Systems, Mountain View, CA) or Canvas X (ACD Systems, Miami, FL) was used to automatically adjust the levels of differential interference contrast images (using the "autolevel" function), to match the dynamic range of fluorescence images to that of the computer display, and to merge differential interference contrast with fluorescence data. All images for a given experiment were processed identically, no signal was excluded by the setting of thresholds, and gamma settings were not altered.

U937 cell adhesion assay

Cell adhesion to immobilized proteins was conducted as previously described with certain modifications.[21] After 96-well plates (Maxisorp; Nalge Nunc International, Rochester, NY) were coated with 10 μg/mL recombinant P-selectin (or 1% BSA) and blocked with 1% BSA (Calbiochem, San Diego, CA) in DPBS, U937 cells suspension in RPMI 1640 medium, with or without the indicated concentrations of anti–P-selectin antibody, were added to the protein-coated wells and incubated for 1 hour at 37°C. Wells were washed 3 times with DPBS, and remaining cells were fixed with 2% formaldehyde for 15 minutes and then stained with 0.2% crystal violet (Sigma-Aldrich) in 2% ethanol for 15 minutes. After 3 washes with water, adherent cells were solubilized with 1% sodium dodecyl sulfate for 30 minutes. Optical density of the wells at 562 nm was read with a microplate reader (Molecular Devices, Sunnyvale, CA). Samples were analyzed in quadruplicate.

Immunoelectron microscopy

HUVECs were grown on 3 × 3 mm glass coverslips in preparation for immunolabeling, freeze-drying, and platinum replication. Cultures were stimulated for various durations (1-10 minutes) with 100 μM histamine in a mammalian Ringer solution at 37°C with gentle rocking to create a low level of fluid shear stress, rinsed briefly in mammalian Ringer solution, and fixed for 30 minutes at room temperature with 2% formaldehyde in fixation buffer (30 mM *N*-2-hydroxyethylpiperazine-*N*′-2-ethanesulfonic acid, pH 7.4, 100 mM NaCl, and 2 mM $CaCl_2$). Fixed cells were rinsed with fixation buffer for 15 minutes and then quenched for 30 minutes with fixation buffer containing 50 mM lysine, 50 mM glycine, and 50 mM NH_4Cl. Cells were rinsed again for 10 minutes and blocked for 30 minutes with 1% BSA in fixation buffer. Coverslips were placed on a wax surface and overlaid for 30 minutes with 25 μL polyclonal rabbit anti-VWF antibody diluted at 1:500. Unattached primary antibody was removed by 3 washes, and coverslips were overlaid for 30 minutes with antirabbit antibody conjugated to 12-nm gold diluted at 1:15. Coverslips were washed, refixed with 2% glutaraldehyde to stabilize the immunolabeling, rinsed multiple times in distilled water, and quick-frozen by forceful impact against a copper block cooled to 4°C with liquid helium. Platinum replicas were made and images were acquired as previously described.[22]

Flow cytometry

Cells were detached from tissue culture dishes with trypsin/EDTA, resuspended at 10^6/mL in DPBS containing 3% fetal bovine serum (Invitrogen) and 2% BSA (Calbiochem), and incubated for 30 minutes on ice. Primary antibody (mouse antihuman $\alpha_v\beta_3$, LM609), diluted to 20 μg/mL in blocking buffer (2% BSA in DPBS), was incubated with cells for 45 minutes at 4°C. Cells were then washed twice with DPBS and resuspended in blocking buffer containing 20 μg/mL secondary antibody conjugated to Alexa Fluor 632 (Invitrogen). After 45 minutes of incubation on ice, cells were washed twice with DPBS, resuspended in 0.3 mL 2% paraformaldehyde in DPBS, and analyzed on a FACSCalibur benchtop analyzer (BD Biosciences, San Jose, CA).

RNA interference

Lentivirus vectors pFLRu-N-Flag and pFLRu-shLuc were provided by Dr Gregory Longmore (Washington University, St Louis, MO). The latter construct contains shRNA sequence targeting firefly luciferase. A short hairpin RNA (shRNA) expression cassette was constructed by polymerase chain reaction (PCR). We chose 3 targeting sequences for human integrin α_v. They are named after the position of their starting nucleotide in the α_v

cDNA sequence (GenBank accession number NM_002210):[23] #576, GCAACAGGCAATAGAGATTAT; #1129, GGAAGAACATGTCCTCCTTAT; #3432 GCTACATCTTGACCCACTAGA. Human U6 promoter (f1) was amplified from a pBS-hU6-1 template[24] using the following PCR primers: 5′ primer, AGAGAATTCTAGAACCCCAGTGGAAAGACGCGCAG; 3′ primer, GGTGTTTCGTCCTTTCCACAAG. The shRNA fragment (f2) was amplified with the following primers: 5′ primer, GTGGAAAGGACGAAACACC+α_V targeting sequence +*TTCAAGAGA*ATAAG; 3′ primer, TCCAGCTCGAGAAAAA+α_V targeting sequence +*TCTCTTGAA*ATAAT. Italicized nucleotides are hairpin sequences. After gel purification of f1 and f2, a PCR was performed with hU6 forward primer, shRNA reverse primer, and mixed template (2 μL purified f1 and f2). The PCR products were purified, digested with *Xba*I and *Xho*I, and subcloned into the pFLRu-N-Flag vector.

Lentivirus generation and transduction

For lentivirus production, a previous protocol[25] was followed with certain modifications. Briefly, subconfluent 293T cells were transfected with packaging plasmids pHR′8.2 deltaR/pCMV-VSV-G at a ratio of 8:1 using 5 μg total packaging plasmid DNA (plasmids were provided by Dr Sheila Stewart, Washington University, St Louis, MO) and 5 μg of pFLRu plasmid. At 24 hours after transfection, the cell culture medium was changed, and on the next day medium containing virus was harvested and passed through a 0.45-μm filter to remove cellular debris. To infect target cells, virus was mixed with an equal volume of fresh medium and protamine sulfate (Sigma-Aldrich) at a final concentration of 10 μg/mL. Cells were washed and incubated with virus mixture overnight. The next day, cells were fed with fresh, virus-free medium. After another 24 hours, puromycin was added at 1.5 μg/mL, and infected cells were incubated under selection for 2 weeks before experiments were performed.

Results

Secreted VWF form extended strings on endothelial surfaces at venous and arterial values of shear stress

To better understand how acutely secreted VWF multimers interact with endothelial cells, we observed the dynamics of VWF secretion and deployment on HUVECs surface in real time, using fluorescence microscopy under both static and flow conditions. In several comparisons, we found that HUVECs prepared locally from umbilical cords and early passage HUVECs purchased commercially behaved indistinguishably. On histamine stimulation, confluent HUVEC monolayers released VWF that remained attached to cell surface as disorganized globular and linear densities (Figure 1A). When HUVECs were exposed to laminar flow, VWF molecules formed strings that ran parallel to the direction of flow, and some of the strings extended as long as several hundred micrometers (Figure 1B). VWF strings were also observed when endothelial cells were stimulated with forskolin, a secretagogue that elevates cAMP level (data not shown). Strings rarely formed in the absence of any agonist (0-2 per field), suggesting that agonist-induced strings are composed of ULVWF molecules originally packaged in Weibel-Palade bodies. The occasional VWF strings secreted without agonist stimulation probably reflect a low but significant basal rate of Weibel-Palade body fusion with the plasma membrane.[26] Maximum string density was obtained at intermediate shear stress of between 10 and 20 dyne/cm^2, suggesting that these VWF strings withstand physiologic shear stress but can be dislodged by pathologically high shear stress (Figure 1C).

VWF strings laterally associate to form bundles and networks

To test whether VWF strings were composed of one or multiple VWF multimers, we used quick-freeze, deep-etch electron microscopy to study VWF morphology under higher resolution. HUVECs were stimulated, fixed, labeled with a polyclonal antibody against VWF, and a secondary antibody conjugated with gold particles. Multiple gold-decorated VWF strands were seen spanning adjacent cells (Figure 2A) and VWF strings frequently intertwined with each other to form bundles (Figure 2B) and networks (Figure 2C).

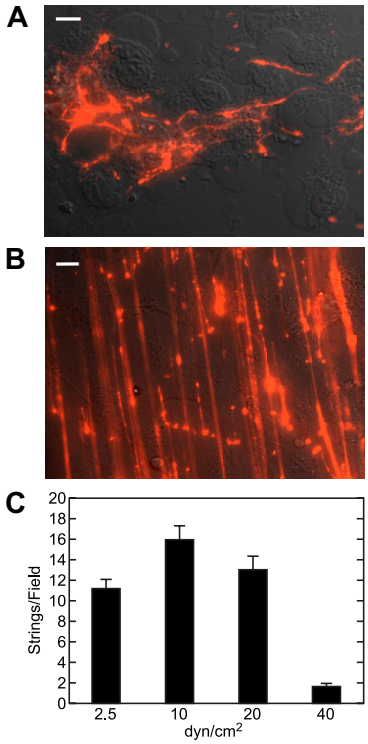

Figure 1. Acutely secreted VWF forms extended strings under fluid shear stress. (A) Confluent HUVECs were stimulated with 100 μM histamine for 30 minutes, washed with DPBS, and fixed with 2% paraformaldehyde without permeabilization. Cell-surface VWF was stained with a polyclonal antibody (A082; Dako North America) and an Alexa Fluor 594–conjugated secondary antibody. Bar represents 10 μm. (B) HUVECs in a parallel plate flow chamber were perfused with medium 199 supplemented with 2% BSA, 100 μM histamine, and fluorescent VWF polyclonal antibody, at a shear stress of 10 dyne/cm^2. Images were captured 5 minutes after the initiation of flow. Bar represents 10 μm. (C) Perfusion assays were conducted at different values of fluid shear stress. The bars indicate the numbers (mean ± SEM) of VWF strings more than 20 μm long formed 5 minutes after the initiation of flow from 10 fields per experiment. Each experiment was performed at least 3 times.

A subset of VWF strings mediates the binding of platelets

Platelets readily bind to VWF on human endothelial cells and form "beads-on-a-string" structures under laminar flow that are visible by phase-contrast microscopy.[5] However, phase-contrast microscopy does not directly detect the VWF but infers the location of VWF strings from the linear arrangement of bound platelets. We therefore compared the distribution of platelets (by phase-contrast) and VWF (by immunofluorescence) after stimulation of HUVECs with histamine and continuous perfusion with buffer containing platelets. Unexpectedly, platelets spontaneously bound to only a subset of VWF strings (Figure 3A). In representative experiments, the percentage of VWF strings that bound platelets was 30%, 35%, and 42% at shear stress of 2.5, 10, and 20 dyne/cm^2, respectively (Figure 3B). Sequential perfusion with platelets followed by fluorescent anti-VWF antibody showed that the anti-VWF labeled all platelet-decorated strings and revealed other strings that had not bound platelets (Figure S2). Therefore, the anti-VWF antibody does not induce the observed heterogeneity in platelet binding by

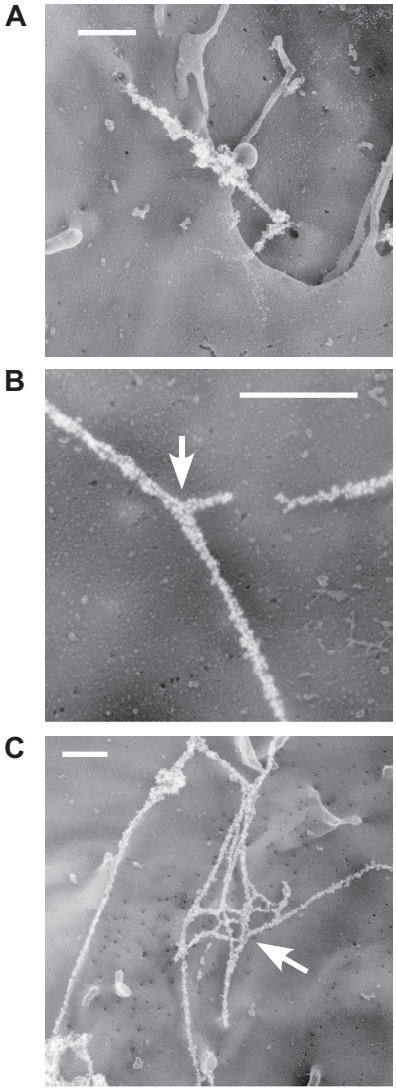

Figure 2. Immunoelectron microscopy of VWF strings. HUVECs were incubated with medium containing 100 μM histamine for 10 minutes with gentle rocking, washed with DPBS, and fixed with 3% paraformaldehyde. Cell-surface VWF multimers were labeled with 12-nm gold-conjugated antibody and visualized by quick-freeze deep-etch electron microscopy. Multiple VWF strands (A) form twisted bundles that sometimes bifurcate (B) and connect with one another to form networks (C). Arrows indicate branching points. Bars represent 500 nm.

displacing bound platelets or inhibiting platelet binding to VWF strings. An anti-GPIbα antibody (6D1) markedly reduced the number of platelet-VWF strings without affecting the total number of VWF strings (Figure 3C), indicating that, as expected,[5] the binding of platelets to VWF strings depended on platelet GPIbα.

VWF strings are stabilized on endothelial cells by discrete anchorage sites

VWF-platelet strings attach to the surface of endothelial cells by relatively few adhesion sites per string.[5,11] Direct visualization by immunofluorescence microscopy indicated that, in the absence of platelets, VWF strings also adhere to endothelial cells through a small number of sites. For example, when the flow direction was reversed, strings collapsed or bent around a few fixed anchorage points. In some cases, new anchorage sites could be recruited as strings moved laterally across the cell surface, yielding curved or tangled strings (Figure 4A). Electron microscopy showed specific

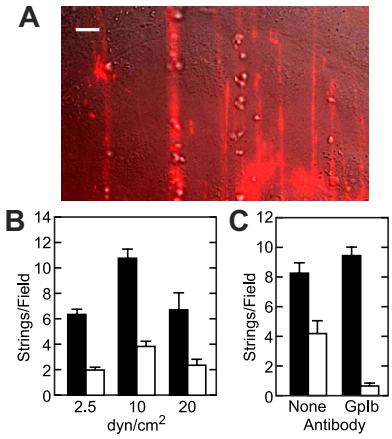

Figure 3. A subset of VWF strings binds platelets. Perfusion assays were performed in the presence of 100 μM histamine, 10^8/mL fixed platelets, and fluorescent VWF polyclonal antibody. (A) A representative image of VWF strings and platelet strings for perfusion assay conducted at 2.5 dyne/cm^2. Bar represents 10 μm. (B) Total fluorescent VWF strings (■) and platelet-decorated VWF strings (□) formed under a fluid shear stress of 2.5, 10, and 20 dyne/cm^2 are shown as the mean plus or minus SEM from 10 fields per experiment. (C) Perfusion assays were performed at a shear stress of 2.5 dyne/cm^2 in the presence or absence of 20 μg/mL antiplatelet GPIbα antibody 6D1. Total fluorescent VWF strings (■) and platelet-decorated VWF strings (□) are shown as mean plus or minus SEM from 10 fields per experiment. Each experiment was repeated at least twice.

contact points of VWF strings with the cell membrane, as indicated by arrows (Figure 4B). Viewing 3-dimensional electron microscopic images indicated that such direct contacts were limited in number and were quite often found at small membrane extensions such as microvilli or ruffles.

P-selectin and VWF string formation

A previous study reported that the binding of platelet-decorated VWF strings to endothelial cells was inhibited by anti–P-selectin antibodies or by recombinant soluble P-selectin. In addition,

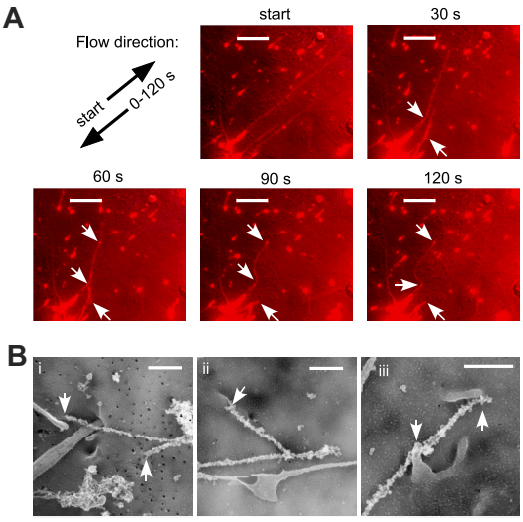

Figure 4. VWF strings attach to HUVECs by discrete adhesion sites. (A) HUVECs were stimulated with histamine and exposed to laminar flow at a shear stress of 2.5 dyne/cm^2. After 5 minutes, flow direction was reversed and images were captured every 30 seconds. indicate the initial flow direction (start) and the reversed flow direction (0-120 s). indicate anchorage sites for VWF strings. Bars represent 20 μm. (B) Electron micrographs of immunogold-labeled VWF strings. Samples were prepared as described in "Immunoelectron microscopy." Arrows indicate cell extrusions in direct contact with VWF strings. Bars represent 500 nm.

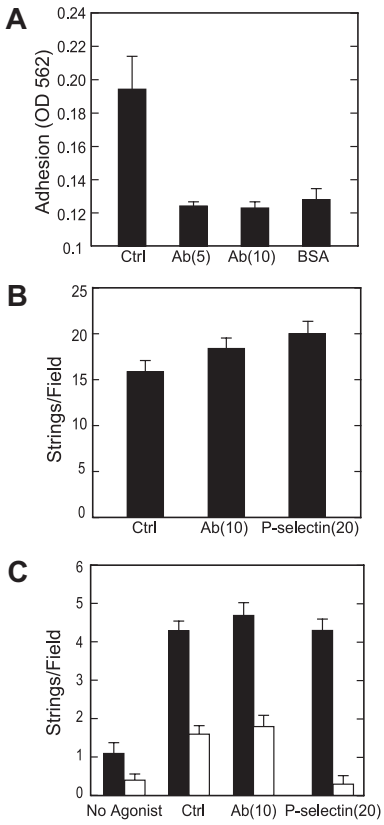

Figure 5. P-selectin and VWF string formation. (A) Wells in an enzyme-linked immunosorbent assay plate were coated with either 20 μg/mL purified P-selectin (R&D Systems) or 1% BSA. U937 cells, which express P-selectin ligand PSGL-1, were resuspended at 10^6/mL, preincubated with buffer (Ctrl) or a polyclonal antibody against P-selectin (Ab) at 5 μg/mL or 10 μg/mL, and adhesion assays were performed as described in "U937 cell adhesion assay." Results indicate the mean plus or minus SD for quadruplicate wells. (B) Perfusion assays were performed at a shear stress of 2.5 dyne/cm^2. Numbers of VWF string formed under control conditions (Ctrl), with P-selectin antibody (Ab), or with purified P-selectin (P-selectin) at the indicated concentrations (μg/mL) are shown. (C) Perfusion assays were conducted in Ca^{2+}- and Mg^{2+}-free DPBS at a shear stress of 2.5 dyne/cm^2, and the numbers of VWF strings (■) and platelet-decorated VWF strings (□) are shown as the mean plus or minus SEM from 10 fields per experiment. Cells were treated with no agonist, or with 100 μM of histamine in the absence (Ctrl) or presence of anti–P-selectin antibody (Ab) or soluble P-selectin at the indicated concentrations (μg/mL). Each experiment was performed 3 times.

immunofluorescence microscopy showed that P-selectin colocalized with cell-associated VWF strings.[11] We also observed that stimulated HUVECs stained with fluorescently labeled anti–P-selectin antibody exhibit punctate immunofluorescence for P-selectin that occasionally colocalizes with VWF strings (Figure S3). These findings suggest that P-selectin anchors VWF on the cell surface. However, under our conditions, in the absence of platelets, neither P-selectin nor anti–P-selectin antibody reduced the number of VWF strings (Figure 5B). Similar results were obtained in the presence of platelets; neither P-selectin nor anti–P-selectin antibody reduced the number of platelet-decorated VWF strings (data not shown). Control studies confirmed that anti–P-selectin antibody prevented the adhesion of U937 monocytic cells to recombinant P-selectin, as expected (Figure 5A), and also inhibited the binding of cells expressing P-selectin (CHO-P cells) to immobilized VWF (Figure S4). These data suggest that P-selectin may not anchor VWF strings on endothelial cells. Alternatively, exogenous inhibitors may not easily disrupt a stable interaction between VWF and P-selectin, which may form during the packaging of both molecules into Weibel-Palade bodies.[10]

The differences between our results and those of Padilla et al[11] probably reflect differences in experimental conditions. For example, we used a perfusion buffer that contained approximately 2 mM Ca^{2+} and 1 mM Mg^{2+}, whereas Padilla et al[11] used divalent cation-free Tyrode's buffer. Because Ca^{2+} and Mg^{2+} cooperatively enhance ligand binding to P-selectin,[21] variations in these cation concentrations may alter the sensitivity of VWF strings to disruption by specific inhibitors. Indeed, when HUVECs were stimulated with histamine in Ca^{2+} and Mg^{2+}-free Tyrode buffer, the inclusion of soluble P-selectin decreased the number of adherent platelet-decorated VWF strings but not the total number of VWF strings (Figure 5C). In this experiment, anti–P-selectin antibody did not reduce the either the total number of VWF strings or the number of platelet-decorated VWF strings. These results suggest that P-selectin–dependent platelet binding to VWF strings depends on divalent cations.

In addition, the total number of strings observed in Ca^{2+} and Mg^{2+}-free Tyrode buffer (Figure 5C) was much lower than the number observed with Ca^{2+} and Mg^{2+} present (Figure 5B). This result is consistent with the known role of extracellular Ca^{2+} ions in the exocytosis of Weibel-Palade bodies after stimulation of endothelial cells with histamine and other agonists.[27,28]

RGDS peptide and anti-integrin $\alpha_v\beta_3$ antibody inhibit VWF string formation

Immobilized VWF binds purified integrin $\alpha_v\beta_3$[29,30] and supports the adhesion of HUVECs through integrin $\alpha_v\beta_3$ in an RGDS-dependent manner,[31,32] which suggests that VWF strings could bind to integrin $\alpha_v\beta_3$ on the endothelial surface. Indeed, either RGDS peptide (Figure 6A) or function blocking anti-$\alpha_v\beta_3$ antibody LM609 (Figure 6B) reduced the number of VWF strings in a dose-dependent manner. In contrast, the CS-1 peptide of fibronectin, which binds to integrin $\alpha_4\beta_1$ and blocks $\alpha_4\beta_1$-dependent cell adhesion,[33] had no effect on VWF string formation (Figure 6A). In addition, antibody CBL497 against integrin $\alpha_5\beta_1$ did not significantly alter VWF string formation (Figure 6C), and neither did antibody LM142 against integrin α_v, which does not block cell adhesion (Figure 6D).

When similar experiments were performed in Ca^{2+} and Mg^{2+}-free Tyrode buffer, we found that RGDS was a less potent inhibitor of VWF string adhesion to HUVECs (Figure 6E), and anti-$\alpha_v\beta_3$ antibody LM609 no longer displaced VWF strings, with or without bound platelets (Figure 6F). Thus, integrin $\alpha_v\beta_3$–dependent adhesion of VWF strings to HUVECs depends on the presence of physiologic divalent cations.

Localization of integrin αv on newly secreted VWF strings

The cell-surface localization of VWF and integrin $\alpha_v\beta_3$ was examined by immunofluorescence microscopy of HUVEC monolayer exposed to histamine under laminar flow at a shear stress of 2.5 dyne/cm^2 for 5 minutes. Integrin α_v is localized to intercellular junctions and also decorates VWF strings (Figure 7; additional examples in Figure S5). Note that α_v signal occurs in a patchy distribution along the length of VWF strings; α_v was not detected at the origin or the distal end of VWF strings.

Reducing the expression of integrin αv on HUVECs impairs VWF string formation

To determine whether integrin $\alpha_v\beta_3$ is necessary to stabilize VWF strings on the surface of HUVECs, we used RNA interference to

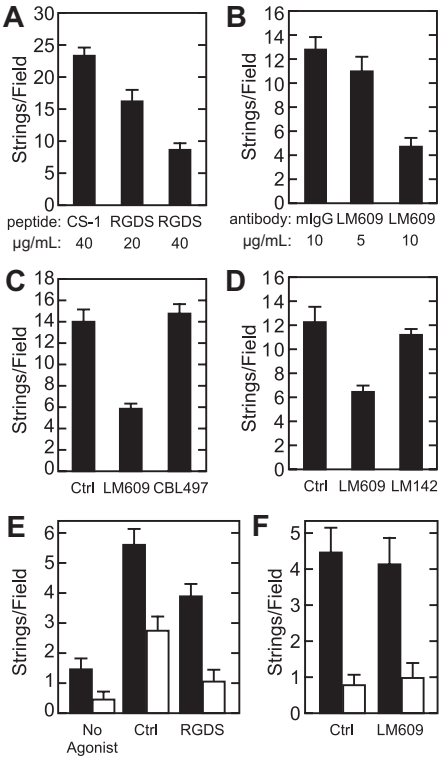

Figure 6. Integrin $\alpha_v\beta_3$ is important for VWF string adhesion. (A) Confluent HUVECs in a flow chamber were perfused at a shear stress of 2.5 dyne/cm^2 using medium 199 supplemented with 100 μM histamine, 2% BSA, and the indicated concentration of fibronectin CS-1 peptide or RGDS peptide, and the number of VWF strings formed was quantified by immunofluorescence microscopy. (B) Perfusion assays were performed similarly with the indicated concentrations of mouse IgG (mIgG) or anti-integrin $\alpha_v\beta_3$ antibody LM609, which blocks ligand binding. (C) Perfusion assays were performed similarly without (Ctrl) or with 10 μg/mL anti-integrin $\alpha_v\beta_3$ antibody LM609 or function blocking anti-integrin α5 antibody CBL497. (D) Perfusion assays were conducted without (Ctrl) or with 10 μg/mL anti-integrin $\alpha_v\beta_3$ antibody LM609 (which blocks ligand binding) or LM142 (which does not block ligand binding). (E,F) Cells were perfused with Ca^{2+}- and Mg^{2+}-free DPBS (E) without (No Agonist) or with 100 μM histamine in the absence (Ctrl) or presence of RGDS peptide (40 μg/mL), or (F) without (Ctrl) or with anti-integrin $\alpha_v\beta_3$ antibody LM609 (10 μg/mL), and total VWF strings (■) and platelet-decorated VWF strings (□) were quantitated. Results are shown as the mean plus or minus SEM from 10 fields per experiment. Each experiment was performed 3 times.

knock down the expression of this integrin. We chose a lentivirus-mediated approach because it can induce sustained gene silencing in a broad spectrum of cell types, including endothelial cells.[24,34,35] Three integrin α_v targeting sequences were designed and cloned into the pFLRu vector, and one of them (sh1129) caused a 70% reduction of $\alpha_v\beta_3$ expression on HUVECs after 2 weeks of selection, as demonstrated by flow cytometry (Figure 8A). HUVECs infected with lentivirus containing the other 2 α_v targeting sequences did not survive the selection. Compared with control cells, which were infected with a lentivirus containing firefly luciferase targeting sequence (shLuc), HUVECs infected with sh1129 had a similar number of Weibel-Palade bodies (Figure S6) but significantly reduced ability to support VWF string anchorage. The number of foci that stained intensely for VWF at the plasma membrane was comparable for shLuc and sh1129 cells, indicating that sh1129 cells could secrete VWF normally but could not retain it on the cell surface (Figures 8B,C). In multiple experiments, shRNA-mediated knockdown of $\alpha_v\beta_3$ expression reduced VWF strings an average of 75.3% at 2.5 dyne/cm^2 and 81.6% at 7.5 dyne/cm^2. Shear forces greater than approximately 10 dyne/cm^2 caused the detachment of sh1129-infected HUVECs, probably because the reduced expression of $\alpha_v\beta_3$ weakened cell adhesion to the substratum.

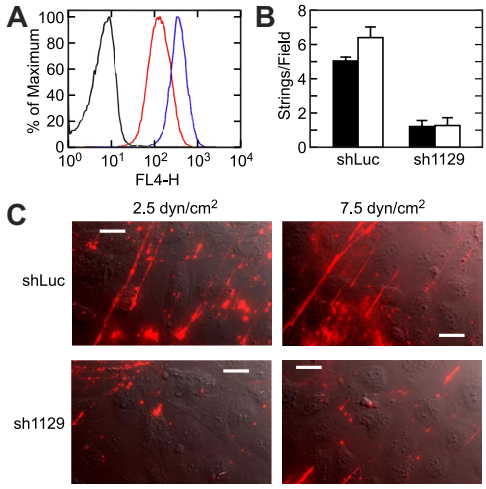

Figure 8. VWF string formation depends on integrin α_v expression. HUVECs were infected with control shRNA lentivirus (shLuc) or integrin α_v shRNA lentivirus (sh1129) and cultured for 2 weeks under selection with puromycin. (A) Fluorescence-activated cell sorter analysis was performed with control antibody on cells treated with shLuc (black trace) or with anti-integrin $\alpha_v\beta_3$ antibody LM609 on cells treated with shLuc (blue trace) or sh1129 (red trace). The level of integrin $\alpha_v\beta_3$ was reduced 70% in sh1129 cells. (B) Lentivirus-infected HUVECs were stimulated with histamine and exposed to fluid shear stress of 2.5 dyne/cm^2 (■) or 7.5 dyne/cm^2 (□). VWF strings were stained in situ with fluorescent anti-VWF antibody and counted. Values represent the mean plus or minus SEM from 10 fields per experiment. (C) Representative images are shown. Flow direction is from bottom left to top right. Bars represent 20 μm.

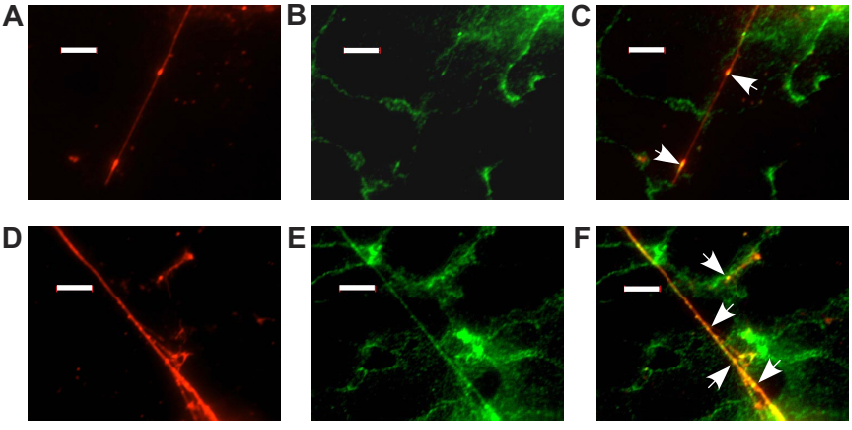

Figure 7. Integrin α_v decorates acutely secreted VWF strings. Confluent HUVECs in a flow chamber were stimulated with 100 μM histamine at 2.5 dyne/cm^2 shear stress for 5 minutes, fixed, and incubated with anti-VWF and anti-integrin $\alpha_v\beta_3$ antibodies as described in "Immunofluorescence microscopy." Panels show immunofluorescence for VWF (A,D) and integrin $\alpha_v\beta_3$ (B,E) with corresponding fluorescent antibodies. Merged images are shown in panels C and F. Arrows indicate selected examples of the colocalization of VWF and integrin $\alpha_v\beta_3$. Bars represent 10 μm.

Discussion

By immunofluorescence microscopy of living HUVECs, we found that VWF strings form and adhere to the cell surface over a broad range of physiologic fluid shear forces, even in the absence of platelets (Figure 1). As reported previously for platelet-decorated VWF strings,[5] VWF strings form readily on activated endothelial cells at relatively low fluid shear forces (eg, 2.5 dyne/cm^2). In contrast, soluble plasma VWF binds immobilized collagen to form a filamentous network only at a much higher fluid shear stress of approximately 20 dyne/cm^2.[36] This disparity probably reflects structural differences between ULVWF stored in Weibel-Palade bodies and VWF in the circulation. Plasma VWF typically has a disorganized globular shape in solution with a maximum dimension of less than 1 μm, and relatively high shear forces are needed to unfurl this globular VWF conformation into an extended filament.[37] In contrast, ULVWF within Weibel-Palade bodies is organized into helical tubules that are stabilized at low pH.[7,38] Fusion of Weibel-Palade bodies with the plasma membrane exposes their contents to the neutral pH of the blood, which facilitates the orderly extrusion of very long VWF strings that attach to the cell surface before they can collapse into a globular conformation with much lower binding affinity.

Unexpectedly, we found that only a subset of newly secreted VWF strings supports stable platelet adhesion (Figure 3), suggesting that some strings may be more hemostatically active than others or that platelet binding could be cooperative. Furthermore, there is a slight increase in the ratio of platelet strings to VWF strings (12%) as the fluid shear stress was increased from 2.5 dyne/cm^2 to 20 dyne/cm^2 (Figure 3B), suggesting that potential platelet-binding sites might be buried inside VWF strands that formed twisted bundles. These sites may be exposed by changing the way individual VWF molecules associate with each other, either through elevated shear stress acting directly on VWF strings or through stretching of VWF strings by bound platelets. In contrast to VWF in solution, which is relatively resistant to ADAMTS13, VWF strings were cleaved rapidly in situ on the endothelial surface (Figure S7). The susceptibility of VWF strings to cleavage by ADAMTS13 may provide a mechanism to quickly reduce the length of VWF multimers and limit the size of platelet aggregates on endothelial cells in vivo. Using 2 different concentrations of recombinant ADAMTS13, we found that platelet-decorated and platelet-free VWF strings were cleaved to a similar extent after 5 minutes (Figure S7). Therefore, in contrast to plasma VWF,[39] platelet binding to extended VWF strings attached to endothelial cells does not substantially increase the rate of cleavage by ADAMTS13, at least at 2.5 dyne/cm^2 fluid shear stress.

VWF strings secreted by HUVECs often are several hundred micrometers long (Figure 1) and can be as long as several millimeters.[5] A structural model for the intracellular storage of VWF suggests that each of the many VWF tubules extending the entire length of a 5-μm Weibel-Palade body could correspond to a single 250-μm VWF multimer.[38] If 250 μm is a rough upper limit for the length of a VWF multimer, then longer VWF strings on endothelial cells are probably constructed by staggered self-association of several VWF multimers.

Evidence for VWF self-association has been described previously.[36,40] For example, reversible homotypic interactions between soluble and immobilized VWF multimers can mediate platelet adhesion under fluid shear stress.[40] At very high levels of shear stress, VWF multimers can form a network of multistranded bundles on a collagen matrix[36] or aggregate irreversibly in solution,[41] possibly by forming new intersubunit disulfide bonds.[42,43] At levels of fluid shear stress too low to induce VWF self-association on other surfaces[36,40] or in solution,[41,42] we have observed that acutely secreted VWF molecules self-associate in diverse patterns, forming twisted bundles and networks on endothelial cells (Figure 2). These multistranded structures may enhance the stability of VWF molecules on endothelial surfaces and probably account for the extreme length of some VWF strings.

VWF strings are anchored and stabilized on endothelial cells by relatively few high-affinity contacts (Figure 4A) that withstand a range of physiologic shear forces (Figures 1C,3A). Electron microscopy shows that VWF strings make direct contact with membrane protrusions at their termini and along their length (Figure 4B). By immunofluorescence microscopy, VWF strings often can be seen emerging from specific foci on the cell surface, to which they remain attached at full extension (Figure 1B). When perturbed by changing the direction of flow, VWF strings can make new discrete, stable contacts as they drift over the cell surface (Figure 4A). Some contacts coincide with foci that stain intensely for VWF (Figure 4A), and others colocalize with punctate concentrations of integrin $\alpha_v\beta_3$ (Figure 7). Cell-surface binding of VWF strings is inhibited by RGDS peptide, by anti-integrin $\alpha_v\beta_3$ antibody LM609 (Figure 6), or by RNA knockdown of integrin α_v (Figure 8). These results indicate that integrin $\alpha_v\beta_3$ is involved in the adhesion of VWF strings to human endothelial surfaces.

In contrast to our results, Padilla et al[11] found that P-selectin, but not integrin $\alpha_v\beta_3$, contributed to the attachment of VWF-platelet strings to endothelial cells. However, this apparent discrepancy appears to be explained by differences in experimental conditions. Ligand binding to integrin $\alpha_v\beta_3$ and P-selectin depends on divalent cations,[21,44,45] and changing the concentrations of Ca^{2+} and Mg^{2+} can selectively alter the dependence of VWF or platelet binding on these adhesive proteins. Under physiologic conditions, with Ca^{2+} and Mg^{2+} present, the attachment of VWF strings to HUVECs involves integrin $\alpha_v\beta_3$ (Figure 6A-D), but without divalent cations the attachment of VWF appears to be independent of integrin $\alpha_v\beta_3$ (Figure 6E,F). Conversely, soluble P-selectin does not affect VWF strings when Ca^{2+} and Mg^{2+} are present (Figure 5B) but impairs platelet binding to VWF strings when these divalent cations are absent (Figure 5C). Therefore, it is possible that both P-selectin and integrin $\alpha_v\beta_3$ contribute to VWF-endothelial interactions.

Our results and those of Padilla et al,[11] using cultured human endothelial cells, differ from those obtained by intravital microscopy in mice. After infusing inhibitory anti-ADAMTS13 antibody to slow the proteolysis of VWF strings, stimulation with histamine resulted in the formation of long platelet-decorated VWF strings adhering to mesenteric venules. The length, number, and persistence of these strings were the same in wild-type, β3-deficient, or P-selectin–deficient mice.[12] These results indicate that platelet-VWF strings can adhere to endothelial cells at low values of shear stress typical of venules, independent of β_3 integrins or P-selectin. However, the continued accumulation of platelets on VWF strings eventually leads to the detachment of these platelet-VWF strings, even at venular shear stress in mice.[12] In contrast, platelet-VWF strings on HUVECs can resist much higher values of shear stress (eg, 20 dyne/cm^2) that may occur in arterioles (Figure 3A).[5] The greater resistance to shear stress for VWF strings on HUVECs would be consistent with binding to additional adhesive molecules, such as P-selectin and integrin $\alpha_v\beta_3$. In addition, cells expressing integrin $\alpha_v\beta_3$ can adhere specifically to surfaces coated with

VWF,[46] and VWF can bind and recruit P-selectin into the membranes of Weibel-Palade bodies.[10] These findings indicate that VWF can interact with integrin $\alpha_v\beta_3$ or P-selectin on cultured endothelial cells, although the circumstances may be quite distinct from those of VWF strings on vascular endothelium in vivo where VWF binding to the cell surface might be mediated in part by other, yet unidentified, adhesive molecules. Further study will be required to determine the impact of binding to integrin $\alpha_v\beta_3$, P-selectin, or other molecules in various pathologic conditions, especially those in which the activities of adhesion receptors or hydrodynamic flow patterns are affected.

Acknowledgments

The authors thank Dr Yunfeng Feng for providing lentiviral vector and advice on RNA interference, Dr Jing-Fei Dong for help with the parallel plate perfusion chamber, and Drs Rodger P. McEver, Barry S. Coller, and Patricia Anderson for providing P-selectin antibodies, platelet GpIb antibody, and purified recombinant ADAMTS13, respectively. Flow cytometry was performed in the Flow Cytometry Facility in the laboratory of Dr Wayne Yokoyama (Washington University).

This work was supported in part by National Institutes of Heath grants HL72917 and HL89746 (J.E.S.) and GM029647 (J.E.H.).

Authorship

Contribution: J.H. designed and performed research, analyzed and interpreted data, and wrote the manuscript; R.R. performed research; J.E.H. designed research and analyzed and interpreted data; and J.E.S. designed research, analyzed and interpreted data, and wrote the manuscript.

Conflict-of-interest disclosure: J.E.S. is a consultant for Baxter BioSciences and Ablynx. The remaining authors declare no competing financial interests.

Correspondence: J. Evan Sadler, Washington University School of Medicine, 660 South Euclid Avenue, Box 8125, St Louis, MO 63110; e-mail: esadler@im.wustl.edu.

References

1. Ruggeri ZM. The role of von Willebrand factor in thrombus formation. Thromb Res. 2007; 120[Suppl 1]:5-9.
2. Wagner DD. Cell biology of von Willebrand factor. Annu Rev Cell Biol. 1990;6:217-246.
3. Sadler JE. von Willebrand factor: two sides of a coin. J Thromb Haemost. 2005;3:1702-1709.
4. Furlan M, Robles R, Lamie B. Partial purification and characterization of a protease from human plasma cleaving von Willebrand factor to fragments produced by in vivo proteolysis. Blood. 1996;87:4223-4234.
5. Dong JF, Moake JL, Nolasco L, et al. ADAMTS-13 rapidly cleaves newly secreted ultralarge von Willebrand factor multimers on the endothelial surface under flowing conditions. Blood. 2002;100:4033-4039.
6. Dong JF. Cleavage of ultra-large von Willebrand factor by ADAMTS-13 under flow conditions. J Thromb Haemost. 2005;3:1710-1716.
7. Michaux G, Abbitt KB, Collinson LM, Haberichter SL, Norman KE, Cutler DF. The physiological function of von Willebrand's factor depends on its tubular storage in endothelial Weibel-Palade bodies. Dev Cell. 2006;10:223-232.
8. Andre P, Denis CV, Ware J, et al. Platelets adhere to and translocate on von Willebrand factor presented by endothelium in stimulated veins. Blood. 2000;96:3322-3328.
9. Motto DG, Chauhan AK, Zhu G, et al. Shigatoxin triggers thrombotic thrombocytopenic purpura in genetically susceptible ADAMTS13-deficient mice. J Clin Invest. 2005;115:2752-2761.
10. Michaux G, Pullen TJ, Haberichter SL, Cutler DF. P-selectin binds to the D′-D3 domains of von Willebrand factor in Weibel-Palade bodies. Blood. 2006;107:3922-3924.
11. Padilla A, Moake JL, Bernardo A, et al. P-selectin anchors newly released ultralarge von Willebrand factor multimers to the endothelial cell surface. Blood. 2004;103:2150-2156.
12. Chauhan AK, Goerge T, Schneider SW, Wagner DD. Formation of platelet strings and microthrombi in the presence of ADAMTS-13 inhibitor does not require P-selectin or beta3 integrin. J Thromb Haemost. 2007;5:583-589.
13. Jaffe EA, Nachman RL, Becker CG, Minick CR. Culture of human endothelial cells derived from umbilical veins: identification by morphologic and immunologic criteria. J Clin Invest. 1973;52:2745-2756.
14. Sundstrom C, Nilsson K. Establishment and characterization of a human histiocytic lymphoma cell line (U-937). Int J Cancer. 1976;17: 565-577.
15. Cheresh DA, Spiro RC. Biosynthetic and functional properties of an Arg-Gly-Asp-directed receptor involved in human melanoma cell attachment to vitronectin, fibrinogen, and von Willebrand factor. J Biol Chem. 1987;262:17703-17711.
16. Coller BS, Peerschke EI, Scudder LE, Sullivan CA. Studies with a murine monoclonal antibody that abolishes ristocetin-induced binding of von Willebrand factor to platelets: additional evidence in support of GPIb as a platelet receptor for von Willebrand factor. Blood. 1983;61:99-110.
17. Pierschbacher MD, Ruoslahti E. Cell attachment activity of fibronectin can be duplicated by small synthetic fragments of the molecule. Nature. 1984;309:30-33.
18. Akiyama SK, Olden K, Yamada KM. Fibronectin and integrins in invasion and metastasis. Cancer Metastasis Rev. 1995;14:173-189.
19. McEver RP, Martin MN. A monoclonal antibody to a membrane glycoprotein binds only to activated platelets. J Biol Chem. 1984;259:9799-9804.
20. Lorant DE, Patel KD, McIntyre TM, McEver RP, Prescott SM, Zimmerman GA. Coexpression of GMP-140 and PAF by endothelium stimulated by histamine or thrombin: a juxtacrine system for adhesion and activation of neutrophils. J Cell Biol. 1991;115:223-234.
21. Geng JG, Bevilacqua MP, Moore KL, et al. Rapid neutrophil adhesion to activated endothelium mediated by GMP-140. Nature. 1990; 343:757-760.
22. Heuser JE, Reese TS, Dennis MJ, Jan Y, Jan L, Evans L. Synaptic vesicle exocytosis captured by quick freezing and correlated with quantal transmitter release. J Cell Biol. 1979;81:275-300.
23. National Center for Biotechnology Information. www.ncbi.nlm.gov/Genbank. Accessed May 20, 2008.
24. Qin XF, An DS, Chen IS, Baltimore D. Inhibiting HIV-1 infection in human T cells by lentiviral-mediated delivery of small interfering RNA against CCR5. Proc Natl Acad Sci U S A. 2003;100:183-188.
25. Blesch A. Lentiviral and MLV based retroviral vectors for ex vivo and in vivo gene transfer. Methods. 2004;33:164-172.
26. Giblin JP, Hewlett LJ, Hannah MJ. Basal secretion of von Willebrand factor from human endothelial cells. Blood. 2008;112:957-964.
27. Hamilton KK, Sims PJ. Changes in cytosolic Ca2+ associated with von Willebrand factor release in human endothelial cells exposed to histamine: study of microcarrier cell monolayers using the fluorescent probe indo-1. J Clin Invest. 1987;79:600-608.
28. Erent M, Meli A, Moisoi N, et al. Rate, extent and concentration dependence of histamine-evoked Weibel-Palade body exocytosis determined from individual fusion events in human endothelial cells. J Physiol. 2007;583:195-212.
29. Conforti G, Zanetti A, Pasquali-Ronchetti I, Quaglino D Jr, Neyroz P, Dejana E. Modulation of vitronectin receptor binding by membrane lipid composition. J Biol Chem. 1990;265:4011-4019.
30. Marcinkiewicz C, Rosenthal LA, Marcinkiewicz MM, Kowalska MA, Niewiarowski S. One-step affinity purification of recombinant alphavbeta3 integrin from transfected cells: protein expression and purification. 1996;8:68-74.
31. Beacham DA, Wise RJ, Turci SM, Handin RI. Selective inactivation of the Arg-Gly-Asp-Ser (RGDS) binding site in von Willebrand factor by site-directed mutagenesis. J Biol Chem. 1992; 267:3409-3415.
32. Denis C, Williams JA, Lu X, Meyer D, Baruch D. Solid-phase von Willebrand factor contains a conformationally active RGD motif that mediates endothelial cell adhesion through the alpha v beta 3 receptor. Blood. 1993;82:3622-3630.
33. Humphries MJ, Komoriya A, Akiyama SK, Olden K, Yamada KM. Identification of two distinct regions of the type III connecting segment of human plasma fibronectin that promote cell type-specific adhesion. J Biol Chem. 1987;262:6886-6892.
34. Brummelkamp TR, Bernards R, Agami R. A system for stable expression of short interfering RNAs in mammalian cells. Science. 2002;296: 550-553.
35. Makinen PI, Koponen JK, Karkkainen AM, et al. Stable RNA interference: comparison of U6 and H1 promoters in endothelial cells and in mouse brain. J Gene Med. 2006;8:433-441.
36. Barg A, Ossig R, Goerge T, et al. Soluble plasma-derived von Willebrand factor assembles to a

haemostatically active filamentous network. Thromb Haemost. 2007;97:514-526.

37. Schneider SW, Nuschele S, Wixforth A, et al. Shear-induced unfolding triggers adhesion of von Willebrand factor fibers. Proc Natl Acad Sci U S A. 2007;104:7899-7903.
38. Huang RH, Wang Y, Roth R, et al. Assembly of Weibel-Palade body-like tubules from N-terminal domains of von Willebrand factor. Proc Natl Acad Sci U S A. 2008;105:482-487.
39. Shim K, Anderson PJ, Tuley EA, Wiswall E, Sadler JE. Platelet-VWF complexes are preferred substrates of ADAMTS13 under fluid shear stress. Blood. 2008;111:651-657.
40. Savage B, Sixma JJ, Ruggeri ZM. Functional self-association of von Willebrand factor during platelet adhesion under flow. Proc Natl Acad Sci U S A. 2002;99:425-430.
41. Shankaran H, Alexandridis P, Neelamegham S. Aspects of hydrodynamic shear regulating shear-induced platelet activation and self-association of von Willebrand factor in suspension. Blood. 2003; 101:2637-2645.
42. Choi H, Aboulfatova K, Pownall HJ, Cook R, Dong JF. Shear-induced disulfide bond formation regulates adhesion activity of von Willebrand factor. J Biol Chem. 2007;282:35604-35611.
43. Li Y, Choi H, Zhou Z, et al. Covalent regulation of ULVWF string formation and elongation on endothelial cells under flow conditions. J Thromb Haemost. 2008;6:1135-1143.
44. Xiong JP, Stehle T, Zhang R, et al. Crystal structure of the extracellular segment of integrin alpha Vbeta3 in complex with an Arg-Gly-Asp ligand. Science. 2002;296:151-155.
45. Pesho MM, Bledzka K, Michalec L, Cierniewski CS, Plow EF. The specificity and function of the metal-binding sites in the integrin beta3 A-domain. J Biol Chem. 2006;281:23034-23041.
46. Pilch J, Habermann R, Felding-Habermann B. Unique ability of integrin $\alpha_v\beta_3$ to support tumor cell arrest under dynamic flow conditions. J Biol Chem. 2002;277:21930-21938.